ELSEVIER

Thermochimica Acta 269/270 (1995) 575–590

thermochimica acta

Anomalous lattice specific heat of $LiInSe_2$ at low temperatures ☆

E. Gmelin*, W. Hönle

Max-Planck-Institut für Festkörperforschung, Heisenbergstrasse 1, D-70569 Stuttgart, Germany

Received 16 September 1994; accepted 9 June 1995

Abstract

The molar heat capacity at constant pressure of the ternary chalcopyrites $LiInSe_2$ and $CuInSe_2$ have been determined at temperatures from 2 K to 300 K with an adiabatic microcalorimeter. From the low temperature data we derive the following Debye temperatures at 0 K: $\theta_0(LiInSe_2) = 265(10)$ K and $\theta_0(CuInSe_2) = 228(3)$ K. The standard entropies and enthalpies at 298.15 K are calculated by integration of the specific heat curves: $S_0 = 146.6(1.5)\,J\,(mol\,K)^{-1}$ and $H - H_0 = 20.17(0.3)\,J\,K^{-1}$ for $LiInSe_2$, and $S_0 = 158.2(1.6)\,J\,(mol\,K)^{-1}$ and $H - H_0 = 21.32(0.25)\,J\,mol^{-1}$ for $CuInSe_2$. Comparisons are made with previously reported values for the molar heat capaciy of these compounds, measured above 200 K, and with other chalcogenides of the type $A^IB^{III}C^{VI}_2$, with A = Cu, Ag, B = Ga, In and C = S, Se, Te. It is shown that the averaged atomic heat scales to one general curve within 3% for all known chalcogenide compounds except the Li compounds. $LiInSe_2$ displays an excess heat below about 80 K that is represented by a (two-level) Schottky anomaly with an energy splitting of $\Delta/k = 71.4(4)$ K suggesting that the Li atom could reside in a double-well potential. Inspection of previously reported data for $LiInTe_2$ hint at a similar effect in that compound.

Keywords: Chalcogenides (I–III–VI_2 compounds); Low temperature heat capacity; Schottky-type anomaly; Thermodynamic standard functions

1. Introduction

Ternary Chalcogenides $A^IB^{II}C^{VI}_2$ (A = Cu, Ag; B = Al, Ga, In; C = S, Se, Te) form tetrahedrally coordinated semiconductors. These compounds are of interest for appli-

* Corresponding author.

☆ Presented at the 6th European Symposium on Thermal Analysis and Calorimetry, Grado, Italy, 11–16 September 1994.

SSDI 0040-6031(95)02569-3

cation in non-linear optical and photovoltaic devices. The most common crystal structure among chalcogenides is isotypic to $CuFeS_2$ (chalcopyrite) [1]. The compound $CuInSe_2$, investigated here, belongs to the chalcopyrite class. Ternary chalcogenides with tetrahedral coordination are also formed with monovalent alkali metal cations where—in contrast to the monovalent noble metal cations—the bonding, and therefore the electronic properties, is not affected by hybridization between cation d and anion p states. The compound $LiInSe_2$, considered in this paper, (and also $LiInS_2$) crystallizes in the orthorhombic β-$NaFeO_2$ structure which represents a distorted superstructure of the wurtzite lattice, whereas $LiInTe_2$ belongs to the chalcopyrite class [2, 3].

For $CuInSe_2$ the former crystal structure determination has been confirmed recently [4]. Few specific heat measurements exist for the chalcogenides in the literature [5–10]. The data do not always cover the whole range from liquid helium temperature to ambient temperature. Some compounds are not yet investigated, e.g. $AgGaSe_2$, $AgInSe_2$, $AgInSe_2$ and the compounds with B = Al. Two of the studied chalcogenides—where the specific heat has been measured from about 10 K to 300 K—scale excellently to a common curve normalized by the zero-Kelvin Debye temperature [6].

The motivation for the present work was threefold:

— First, to evaluate the influence of the cation (A = Li) in comparison to the cations having energetically high lying d electrons (A = Ag, Cu) which induce a p–d hybridization of the highest valence band whereas Li does not allow a d electron interaction. Eventually an electronic specific heat contribution exists in $CuInSe_2$ at low temperatures.

— Second, to provide experimental evidence for anomalies in the low temperature lattice heat capacity of $LiInSe_2$ which we expected due to the high vibrational anisotropy of the Li atom. In $LiInSe_2$ the Li atom is shifted by ~ 8.8 pm away from the gravicenter of the surrounding tetrahedron, antiparallel to the longest Li–Se bond. Beside that displacement the Li atom exhibits in this crystal structure an extremely elongated and unusual thermal ellipsoid with a r.m.s. displacement of $u = 25$ pm nearly exactly in the direction of the crystallographic a-axis whereas for $CuInSe_2$ a much smaller value of $u = 12.2$ pm is observed. A section of the $LiInSe_2$ structure with the thermal displacement factors is shown in Fig. 1. Also, we wished to know whether $LiInSe_2$ fits into the scaling behaviour of the specific heats of $AgInTe_2$ and $CuInSe_2$ [6].

— Third, to obtain more specific heat data for the chalcogenides in order to make a more comprehensive comparison of the available specific heat, standard entropy and enthalpy data.

In this paper we report on heat capacity measurements $LiInSe_2$ and $CuInSe_2$ using an adiabatic calorimeter in the temperature range 2 K to 300 K. We also extend the analysis of low-temperature specific heat data reported for $LiInTe_2$ [10]. A specific heat curve, generalized with respect to Debye-temperature extrapolated to 0 K, describes well, within about 3%, the molar heat capacity of all chalcogenides.

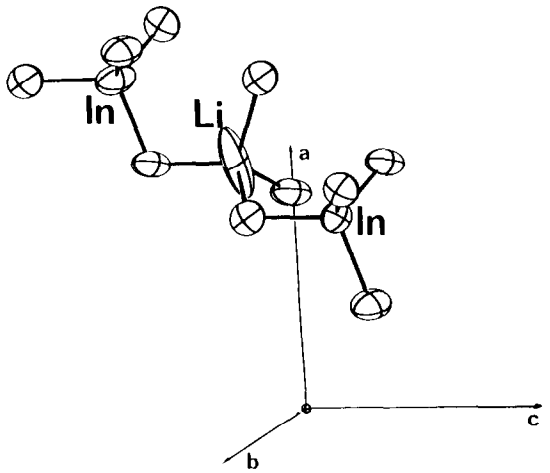

Fig. 1. Section of the $LiInSe_2$ structure with thermal displacement factors (99.9% probability). Note the unusual elongation of the Li atom ellipsoid.

2. Experimental

$LiInSe_2$ was prepared by heating the elements of high purity in sealed quartz ampoules as described earlier [11]. The sample investigated here was identical to that used for the single crystal structure determination [2]. $CuInSe_2$ was synthesized as described elsewhere [12]. Both materials are chemically stable in air. X-ray powder patterns taken from the compounds show that they are single phase. For the calorimetric measurements, the polycrystalline material was first ground in an agate mortar and then pressed into pellets of 6 mm diameter under a force of three tons (without any further heat treatment).

The quasi-adiabatic calorimeters used are especially designed for heat capacity measurements with small samples [13] and with modifications of the electronics described previously [14]. Sapphire plates serve as sample holders [15]. These are equipped either with a commercially available and calibrated germanium resistance thermometer for the low temperature range or with a platinum thermometer used for experiments above 60 K [16, 17]. Both thermometers are calibrated with reference to IPTS-68. In the temperature range of our experiments, conversion from IPTS-68 to ITS-90 introduces negligible errors [18] in both the temperature scale and thermodynamic values. Therefore, we did not attempt to convert our data to ITS-90. The energy given to the sample produced by the heater on the sample holder during each heating-step resulted in temperature increments of $\Delta T/T \approx 2\%$ below 4 K, $\Delta T/T \approx 1.5\%$ up to 20 K and $0.5 < \Delta T/T < 1\%$ for temperatures above 30 K. Application of about 1–2 mg of Apiezon grease ensures good thermal contact between sample holder and sample. The thermal contact within the sample (between grains) must be good since the thermal equilibrium times are determined by the thermal relaxation sample-to-

sample holder via Apiezon N grease. The measured heat capacity is corrected on-line for the precise amount of grease used.

Based on earlier measurements of the heat capacity of a 0.5 g copper sample (T4.4) of Calorimetry Conference Standard, we estimate the absolute accuracy of the specific heat determination for both samples to be $\approx 0.012 C_p$ at temperatures below 30 K, $0.015 C_p$ in the interval $30 < T < 120$ K and again decreasing to $0.012 C_p$ at higher temperatures. The reproducibility of the measurements is much higher. The samples measured had masses of 1.0177 g and 0.9264 g for $LiInSe_2$ and $CuInSe_2$, respectively. The empty calorimetric sample holder contributed about 25% to the total heat capacity at $T = 10$ K, 38% at $T = 50$ K and 35% near room temperature.

3. Results

Fig. 2 gives a plot of the molar heat capacity results $C_p(T)$ for $LiInSe_2$ and $CuInSe_2$ below 100 K as a function of temperature T on a double logarithmic scale. The low temperature range, below 8 K, is shown in Fig. 3 in a plot C_p/T vs. T^2. This representation also displays some of the individual points measured (more than 400 between 2 K and 300 K) that are not resolved in Fig. 2. The variation of the effective Debye temperature $\theta_D(T)$ with temperature obtained by fitting the Debye function to

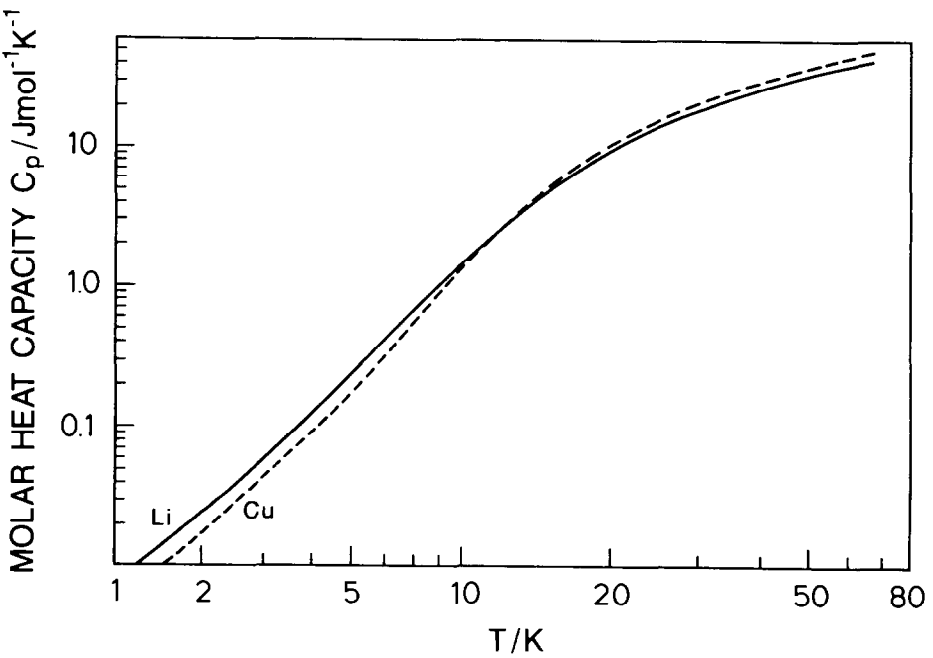

Fig. 2. Molar heat capacity at constant volume C_p of $LiInSe_2$ (——) and $CuInSe_2$ (– – –) as a function of temperature T.

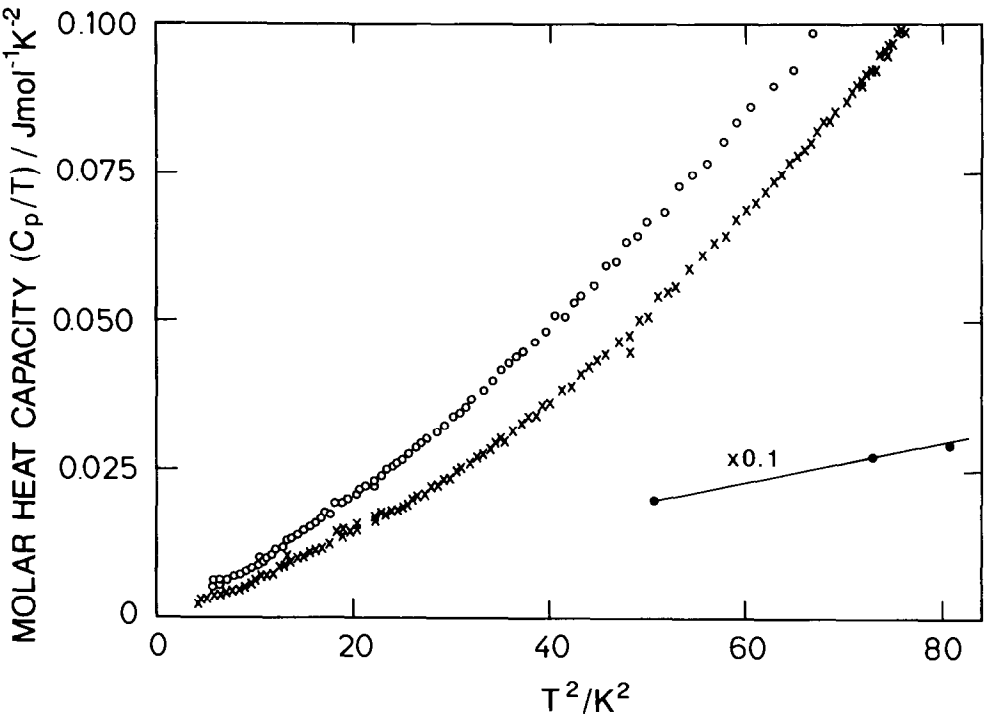

Fig. 3. Low-temperature molar heat capacities C_p/T as a function of temperature T^2 for $LiInSe_2$ (○○○○○) and $CuInSe_2$ (× × × × ×). Values for $LiInTe_2$ (●●●●●)taken from Ref. [10] are shown for comparison.

each specific heat data point, is plotted in Fig. 4. This representation is useless at room temperature since the C_p data approach or exceed Neumann–Kopp's rule. We did not carry out a correction of $(C_p - C_v) = \beta^2 VT/\kappa \approx A(C_p)^2 T$ for the materials considered here because: an estimate of $C_p - C_v$ by using the volume expansion β, the molar volume V, and the adiabatic compressibility κ, yield very small corrective values ($< 0.2\%$) for $T < 300$ K. The experimental specific heat values are fitted to smoothed curves using a polynomial. The standard deviation of the polynomial fitted is less than 0.47%. Table 1 contains values for the standard molar heat capacity, enthalpy, entropy and Gibb's free energy at rounded temperatures. The deduced thermodynamic functions are obtained by integration of the measured specific heats, assuming a Debye–T^3 behaviour at $T < 2.5$ K.

4. Data analysis and discussion

4.1. Low temperature specific heat

The general temperature behaviour of the molar heat capacity, as shown in Fig. 2, is smooth. As expected for both compounds, they do not show any phase transition. A C_p

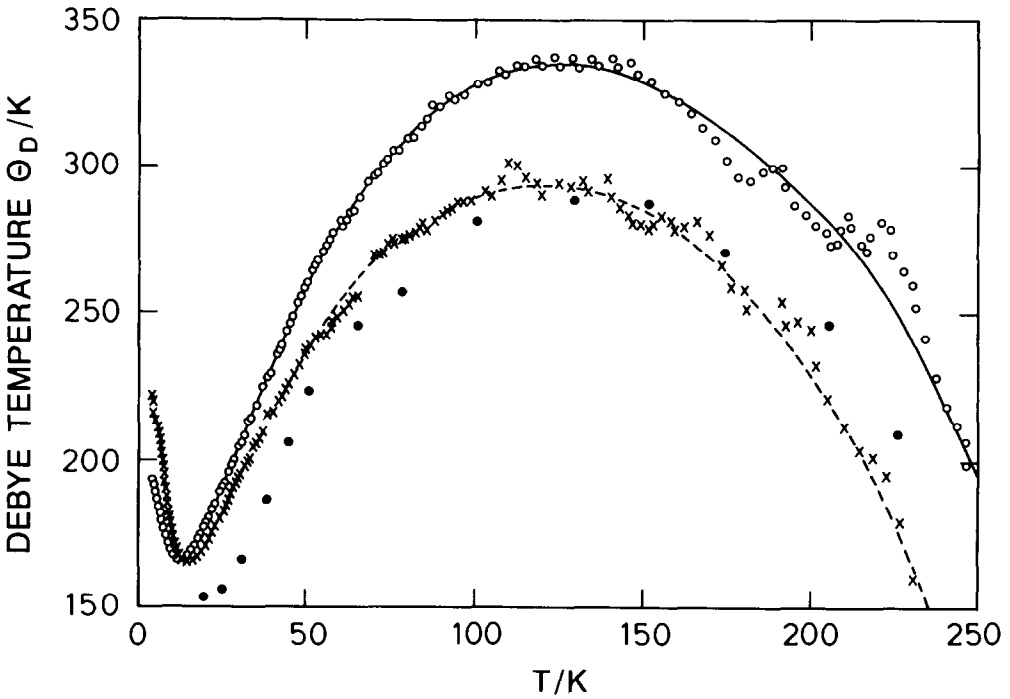

Fig. 4. Debye temperatures of $LiInSe_2$ (○○○○○) and $CuInSe_2$ (× × × × ×) as calculated from the Debye function. Values for $LiInTe_2$ (●●●●●) taken from Ref. [10] are shown for comparison. Continuous and dashed lines are only guidlines to the eye.

Table 1
Smoothed values of standard molar heat capacity C_p and the standard thermodynamic functions enthalpy $H - H_0$ and entropy S for $LiInSe_2$ and $CuInSe_2$. ($R = 8.31451\ J\,(mol\,K)^{-1}$; $M(LiInSe_2) = 279.8\ g\ mol$ and $M(CuInSe_2) = 336.98\ g\,mol^{-1}$)

Temperature, T/K	Molar heat capacity, C_p/J $(mol\,K)^{-1}$	Enthalpy $H - H_0$/J mol^{-1}	Entropy S/J $(mol\,K)^{-1}$
$LiInSe_2$			
2	0	0.004	0.003
3	0.02811	0.03303	0.01483
4	0.05155	0.06982	0.02517
5	0.12511	0.15287	0.04347
6	0.26556	0.34204	0.07758
7	0.48466	0.71019	0.13390
8	0.78979	1.3400	0.21755
9	1.1845	2.3196	0.33248
10	1.6692	3.7390	0.48159
15	5.2909	20.386	1.7822
20	10.171	58.758	3.9562

Table 1 (*Continued*).

Temperature, T/K	Molar heat capacity, C_p/J (mol K)$^{-1}$	Enthalpy $H - H_0$/J mol^{-1}	Entropy S/J (mol K)$^{-1}$
25	15.233	122.39	6.7745
30	19.834	210.28	9.9674
35	23.944	319.88	13.338
40	27.804	449.34	16.789
50	34.533	761.38	23.725
60	40.852	1138.7	30.587
70	46.679	1576.7	37.328
80	52.042	2070.7	43.916
90	56.969	2616.1	50.335
100	61.485	3208.7	56.574
110	65.617	3844.6	62.631
120	69.387	4519.9	68.505
130	72.819	5231.2	74.197
140	75.934	5775.2	79.709
150	78.754	6748.9	85.046
160	81.296	7549.4	90.211
170	83.581	8374.0	95.209
180	85.624	9220.2	100.04
190	87.442	10085.0	104.72
200	89.051	10768.0	109.25
210	90.462	11866.0	113.63
220	91.691	12777.0	117.86
230	92.747	13699.0	121.96
240	93.642	14631.0	125.93
250	94.385	15571.0	129.77
260	94.983	16518.0	133.48
270	95.445	17470.0	137.08
280	75.775	18427.0	140.55
290	95.979	19386.0	143.92
300	96.061	20346.0	147.17
298.15	96.045	20.168	146.57
$CuInSe_2$			
2	0	0.004	0.003
3	0.04499	0.02262	0.00963
4	0.06075	0.07694	0.02516
5	0.08726	0.14790	0.04089
6	0.17033	0.27044	0.06300
7	0.34161	0.51804	0.10084
8	0.62092	0.98970	0.16341
9	1.0184	1.7992	0.25831
10	1.5365	3.0667	0.39137
15	5.6807	20.167	1.7215
20	11.226	62.201	4.1017
25	16.783	132.39	9.2112

Table 1 (*Continued*).

Temperature, T/K	Molar heat capacity, C_p/J (mol K)$^{-1}$	Enthalpy $H - H_0$/J mol^{-1}	Entropy S/J(mol K)$^{-1}$
30	21.899	229.26	10.729
35	26.782	351.00	14.473
40	31.557	496.94	18.363
50	40.148	856.67	26.354
60	47.356	1295.0	34.327
70	53.608	1800.6	42.108
80	52.053	2364.5	49.630
90	63.815	2979.4	56.866
100	68.004	3638.9	63.811
110	71.711	4339.8	70.470
120	75.011	5071.8	76.854
130	77.966	5836.9	82.977
140	80.626	6630.1	88.854
150	83.031	7448.6	94.500
160	85.210	8270.0	99.730
170	87.184	9152.1	105.15
180	88.771	10033.0	110.19
190	90.581	10931.0	115.04
200	92.022	11844.0	119.72
210	93.302	12770.0	124.25
220	94.428	13709.0	128.61
230	95.407	14659.0	132.83
240	96.252	15617.0	136.91
250	96.979	16583.0	140.86
260	99.611	17556.0	144.67
270	98.177	18535.0	148.37
280	98.717	17520.0	151.95
290	99.283	20510.0	155.42
300	99.936	21806.0	158.80
298.15	99.815	21321.0	158.17

curves tend to approximately 100 J(mol K^{-1}) near room temperature according to Neumann–Kopp's rule. The curves increase further linearly due to anharmonicity [8]. The crossing of the specific heats of $LiInSe_2$ and $CuInSe_2$ near 12 K is clearly demonstrated. This behaviour is unusual and inconsistent with the known heat capacities of chalcogenides at low temperatures. According to a general rule, the molar heaty capacity of the material with the lighter molar mass possesses, in isostructural compounds, the higher Debye temperature and lower low-temperature molar heat capacity. This rule is reversed for the two compounds considered here. The excess heat capacity of $LiInSe_2$, which amounts to 30% of the total specific heat when compared with the Cu compound, is interpreted in the next section as a two-level Schottky anomaly resulting from the Li atoms split position.

At low temperatures ($T < 3$ K) the data indicate a linear relationship, as displayed in Fig. 3, which extrapolates to the origin. The contribution of the free carrier—an electronic specific heat—is not detectable. From the slope of the linear part of the curves we calculate the low temperature limiting Debye temperatures $\theta_0(T=0) = 265$ K for $LiInSe_2$ and $\theta_0(T=0) = 229$ K for $CuInSe_2$. Note that the deviation from Debye's T^3-law—linear part of the curves in Fig. 3—occurs for both compounds even at $T > 3$ K. Similar observations have been reported for other chalcogenides [6]. This strong deviation, and consequently the steep decrease of Debye temperatures in the 3 K-to-15 K section in Fig. 4, reflects a high density of low-lying acoustic frequencies for all chalcogenides.

4.2. *Comparison of specific heat of chalcogenides*

Fig. 5 shows a graph of the normalized molar heat capacity of chalcogenides ($C_p\theta_0/12RT$) vs. the reduced temperature T/θ_0. The continuous line represents the averaged molar heat capacity of $CuInSe_2$ and $AgInTe_2$. Some data from the present study are plotted as circles (○) for $LiInSe_2$ and crosses (×) for $CuInSe_2$. We observe a deviation of the calorimetric data of the Li compound for $T < 0.25\theta_0$. The scaling of

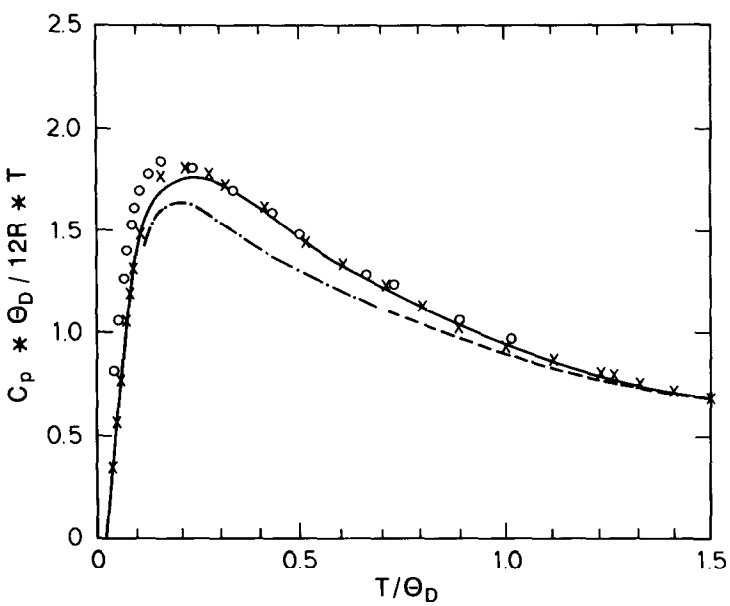

Fig. 5. Specific heat, normalized to Debye temperature θ_0 and high-temperature limiting value $12RT$, vs reduced temperature T/θ_D. Averaged molar heat capacities for two chalcogenides (——)—$AgInTe_2$ and $CuInS_2$—and some data from the present study for $LiInSe_2$ (○○○) and $CuInSe_2$ (× × ×) are plotted; (– – –) represents values taken with a scanning calorimeter and reported in Ref. [8]. Data for $LiIn\ Te_2$, calculated with $\theta_0 = 180$ K, are shown also (–·–·–·–); these values coincide with the averaged curve (——) when $\theta_0 = 205$ K is taken.

the data of all chalcogenides that have considerably different Debye temperatures (see Table 2) to one general curve expresses the identical form of the phonon density of states. The lattice force constants must be nearly identical and only small variations of the atomic distances are involved. The relationship $\theta_0(2)/\theta_0(1) = [a(2)/a(1)][M(1)/M(2)]^{-0.5}$ is strictly valid only for monoatomic or diatomic compounds; a denotes the interatomic distance and M the atomic mass. However, empirically, this relationship holds approximately for most more complex multi-atomic substances [19]. The scaling of the Debye temperature θ_0 with the molecular mass $M^{-0.5}$ is illustrated in Fig. 6. Therein the calorimetrically determined Debye temperatures (at 0 K) for the chalcogenides are located on a straight line. Using the generalized form of the plots in Figs. 5 and 6, we can derive by numerical integration the specific heats and the thermodynamic functions of other chalcogenides, which have not yet been investigated calorimetrically, within error limits of less than 3%. We note that a relationship similar to that shown in

Table 2
Experimental values of Debye temperature at 0 K θ_0, molar heat capacity C_p, standard molar enthalpy $H - H_0$ and entropy S (at 298.15 K) for chalgenides (I–III–VI_2 compounds)

Compound	Ref.[a]	Molar mass/g	θ_0/K	C_p/ J(mol K)$^{-1}$	$H - H_0$/ (J mol^{-1})	S/ J(mol K)$^{-1}$	T range/K
$AgInTe_2$	[6]	477.92	155.9		24.07	198.7	1–300
$CuInTe_2$	[6]	433.58	191.4				1–40
	[7]		195.1(.7)				2–30
	[9]						300–500
$AgGaTe_2$	[6]	432.821	182.4				1–40
$CuGaTe_2$	[7]	388.48	226.2(.7)				2–30
	[9]						300–500
$AgInSe_2$		380.62					
$LiInTe_2$	[8]	377.0	180[b]				200–550
	[10]			101.73	21.76	168.1	7–300
	●		205[c]	101.73	21.67[b]	167.3[b]	7–300
$CuInSe_2$	[6]	336.28	221.9				1–40
	[9]						300–500
	●		228(3)	99.815	21.32(.25)	158.2(1.5)	2–300
$AgGaSe_2$		335.52					–
$CuGaSe_2$	[7]	291.18	262.0(.7)				2–30
$AgInS_2$		286.7					–
$LiInSe_2$	[8]	279.80					200–550
	●		265(10)	96.045	20.17(.3)	146.6(1.5)	2–300
$CuInS_2$	[6]	242.49	273		19.59	137.2	1–300
	[9]						300–500
$AgGaS_2$	[5]	241.73	255				2–40
$CuGaS_2$	[5]	197.39	356				2–40
	[9]						300–600
$LiInS_2$	[8]	185.70					200–550

[a] ●Present work.
[b] Estimate from analysis of high temperature anharmonicity.
[c] Our estimate by evaluating the data given in Ref. [9].

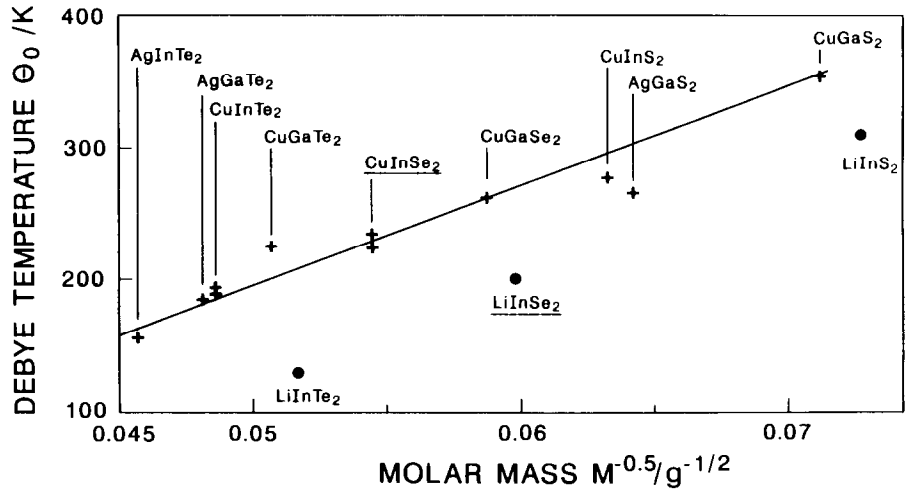

Fig. 6. Scaling of the Debye temperature (at 0 K) θ_0, as determined from calorimetric measurements, with molar mass $M^{1/2}$ for various chalcogenides.

Fig. 6 also holds for the II–IV–V_2 compounds, however, the slope θ_0 vs $M^{-0.5}$ is much steeper.

Table 2 lists the calorimetrically determined Debye temperatures θ_0 of I–II–VI_2 compounds. Estimated Debye temperatures θ_{Tm} and θ_κ calculated from the melting points T_m (Madelung–Einstein relationship) of the chalcogenides or from their microhardness or compressibility, κ, (Lindemann relationship) almost agree within 5% or better with θ_0 (calorimetric). Such values are not given here but are tabulated in Ref. [5] (Table I) and Ref. [6] (Table I). Debye temperatures derived from elastic constants, when these have been measured, almost agree within 3% with the calorimetric ones.

Further values of the specific heat of $LiInSe_2$ measured with a SETARAM DSC-111 scanning calorimeter are indicated in Fig. 5 as a dotted line [8]. These values are in less good agreement with the other data for I–III–VI_2 materials near 80 K. Presumably the deviation originates from systematic errors that easily occur with scanning calorimeters at temperatures far below room temperature. Specific heat results for $LiInTe_2$ reported earlier are also shown, as a point-dotted line [10]. These data disagree with those for the other chalcogenides only apparently because the exact value of the Debye temperature extrapolated to 0 K is not known (lowest measured temperature 8 K). Computation of the lowest measured data point shown in Ref. [10] yields an unexpectively low value of $\theta_0 = 128$ K. A theoretical estimate made in Ref. [9], using an extrapolation from high temperatures, leads to $\theta_0 = 180 \pm 50$ K. The resulting scaled specific heat curve for $LiInTe_2$ is also shown in Fig. 5. Obviously, the Debye temperature $\theta_0(LiInTe_2)$ must be still larger. When $\theta_0 = 205$ K is chosen, the specific heat fits the generalized specific heat curve as displayed in Fig. 5 as a continuous line. Then, for above $T/\theta_0 = 0.4$, the specific heat curve of $LiInTe_2$ lies on the generalized curve of the chalcogenides (continuous line in Fig. 5) within 2%. Below $T/\theta_0 = 0.4$, however, an

excess heat very similar to that found in $LiInSe_2$ develops. The anomalous temperature-dependence of the low temperature specific heat of $LiInSe_2$ and $LiInTe_2$ is also well displayed in Fig. 4. Their temperature-dependent Debye-curves decrease more steeply than the $\theta_D(T)$ curve of $CuInSe_2$ that can be regarded as typical for the chalcogenides. Consequently, the θ_0 values for both Li compounds are found about 30% too low and do not fulfil the θ_0 vs. $M^{-0.5}$ relationships shown in Fig. 6.

4.3. *Schottky anomalies in $LiInSe_2$ and $LiInTe_2$*

According to Figs. 4 to 6 the two Li chalcogenides for which the low-temperature specific heats are known deviate remarkably from the general behaviour of the other chalcogenides. Previous IR experiments on (LiCu)$InSe_2$ mixed crystals hint at a weak Li–C^{VI} bond [20]. The A^I–C^{VI} bond plays a dominant role in anharmonicity effects in these compounds and is particularly noticeable in the Li compounds [8]. The determination of the $LiInse_2$ crystal structure revealed a displacement of the Li atom; it is shifted 8.8 pm out of the centre of the tetrahedra and, in addition, displays unusually anisotropic thermal displacement factors. From this result it was suggested by one of the present authors (W.H.) that Li presumably resides in a split position. This means a double well potential that, in principle, should generate a thermally activated Schottky-type anomaly. Such an anomaly often becomes visible in the specific heat provided that the corresponding potential barrier is not too high ($\Delta E \leq k T_{Sch}$; $T_{Sch} <$ 100 K), so that the peak of the Schottky contribution (maximum 3.64 J (mol K)$^{-1}$) is not masked by the molar lattice heat capacity.

Concerning the structure we assume a split position of the Li atom at low temperatures and compute the observed excess specific heat this way. We show that the specific heat of $LiInSe_2$ is composed of the 'normal' lattice heat of the chalcogenides, as given in Figs. 5 and 6, and a two-level Schottky term. In each moment every lithium atom can occupy only one of the two positions in a double-well. Transitions from one position into another take place either by thermal activation or by tunnelling that is observable only at extremely low temperatures. There will be an equal probability for both sites at sufficiently high temperature ($\Delta E \gg k T$) but the Li atom is trapped in one of the two locations when the thermal energy is reduced below the thermal activation energy ΔE of the two-level system. The activation of the atomic movement in two- or multi-level systems with increasing thermal energy occurs in various materials, e.g. amorphous, ionic conductors, alloys and crystalline substances [21–23]. The presence of a two- or multi-level system is reflected by a characteristic temperature-dependence of an additional specific Schottky anomaly. The Schottky function in its simplest form for a two-level scheme is [24]:

$$C_{Sch} = R(\Delta E/kT)^2 \frac{\exp(\Delta E/kT)}{[1+\exp(\Delta E/kT)]^2}$$

where R denotes the general gas constant. The integral change of molar entropy related to a Schottky anomaly is $\Delta E = R \ln 2$; the maximum of the Schottky specific heat occurs near $T = 0.417 \Delta E/k$ with $C_p = 3.64$ J (mol K)$^{-1}$ for a two-level system. The result of our calculation for $LiInSe_2$ is shown in Fig. 7. It is computed as follows: First,

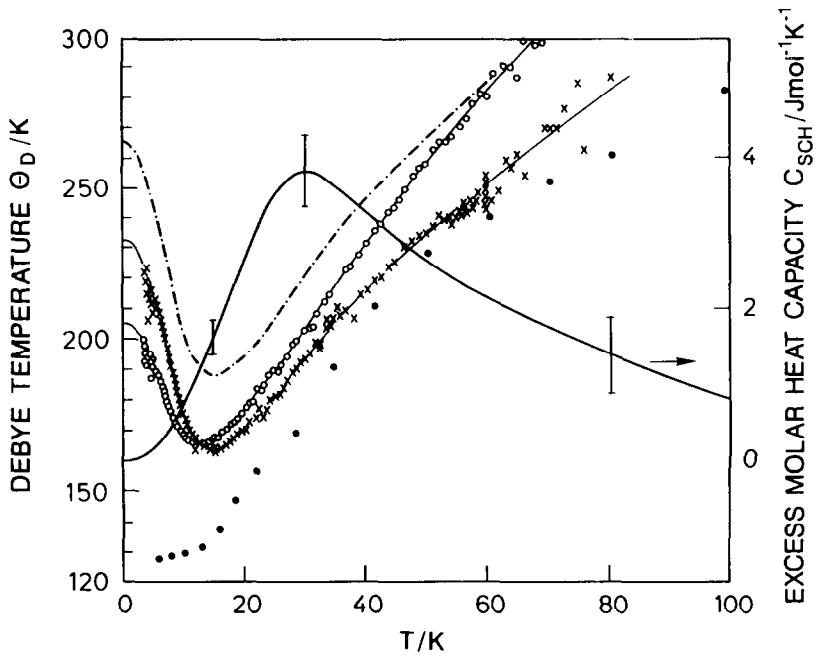

Fig. 7. Debye temperaure $\theta_0(T)$ and excess molar heat as function of temperature T in the low temperature range: (○○○○○)-measured data for $LiInSe_2$, × × × × ×-measured data for $CuInSe_2$, (●●●●●)-values for $LiInTe_2$; data are calculated from Ref. [9], (–·–·–·–)-reconstructed lattice specific heat of $LiInSe_2$ by using $\theta_0 = 265$ K with the generalized curve and relation shown in Figs. 4 and 5. Continuous line curve (——) together with the right hand scale illustrates the specific heat of the two-level Schottky anomaly. The curve is the difference between the meeasured (○○○○○) and the reconstructed (–·–·–·–) molar heat capacities for $LiInSe_2$.

we scale the experimental $\theta_D(T)$ curve (circles in Fig. 7) to the generalized form of specific heat of chalcogenides by using the relationship given in Fig. 6 and the formula mentioned above $\theta_0 \sim M^{-0.5}$. This procedure results in a $\theta_D(T)$ curve plotted as point–dotted line in Fig. 7. It constitutes the reconstructed pure lattice heat C_{latt} of $LiInSe_2$ with $\theta_0 = 265(10)$ K. Second, we calculate from that $\theta_D(T)$ curve the lattice specific heat that turns out to be identical to the generalized specific heat curve as displayed in Fig. 5 as solid line. Third, we deduce C_{latt} from C_{exp}, the experimentally determined specific heat, and take the remaining specific heat as the Schottky term:

$$\Delta C_{Sch} = C_{latt} - C_{exp}$$

The Schottky heat is plotted as a solid line in Fig. 7 (use right side scale) and fits perfectly the theoretical one for a two-level system. The energy splitting amounts to $\Delta E/k = 71.4(3)$ K; consequently, we take the presence of the Schottky anomaly as proof of the existence of the assumed split position for the Li atom in $LiInSe_2$.

It is tempting to inspect similarly the previously reported specific heat of $LiInTe_2$ [8]. A stringent analysis like that for the selenide compound is, unfortunately, not possible

for the telluride compound although, as noted before, hints of a Schottky anomaly exist. The reported data limit the data analysis to about $T > 10$ K. In Fig. 5 the specific heat of $LiInTe_2$ can be brought onto the generalized curve when we use $\theta_0 = 205(15)$ K to agree with the value expected from Fig. 6. Then an excess heat remains below about 60 K that may be attributed to a Schottky anomaly.

We conclude that presumably the Li atom in $LiInTe_2$ also holds a split position similar to that found for $LiInSe_2$ although room temperature investigation of the thermal displacement factors does not indicate an anisotropy like that detected for $LiInSe_2$. Therefore, it remains an open question that could be decided by specific heat measurements below 10 K.

4.4. *Thermodynamic functions*

Table 2 provides a selection of thermodynamic values—Debye-temperature (at 0 K) θ_0, specific heat C_p, enthalpy $H - H_0$ and entropy S at 298.15 K—for the chalcogenides. The temperature ranges of the calorimetric studies are also tabulated. The data are arranged according to decreasing molecular mass M. The interdependence of M and θ_0 has already been shown in Fig. 6. Similar linear relationships are valid for H and $S - S_0$ as a function of θ_0. as is illustrated in Fig. 8. Both plots, Figs. 6 and 8, show that the chalcogenides are very similar in respect of their lattice dynamics. The plots also demonstrate the unique position of the Li compounds. Thus, the total lattice entropy of $LiInSe_2$ is higher than expected compared to the compounds neighboured in molecular

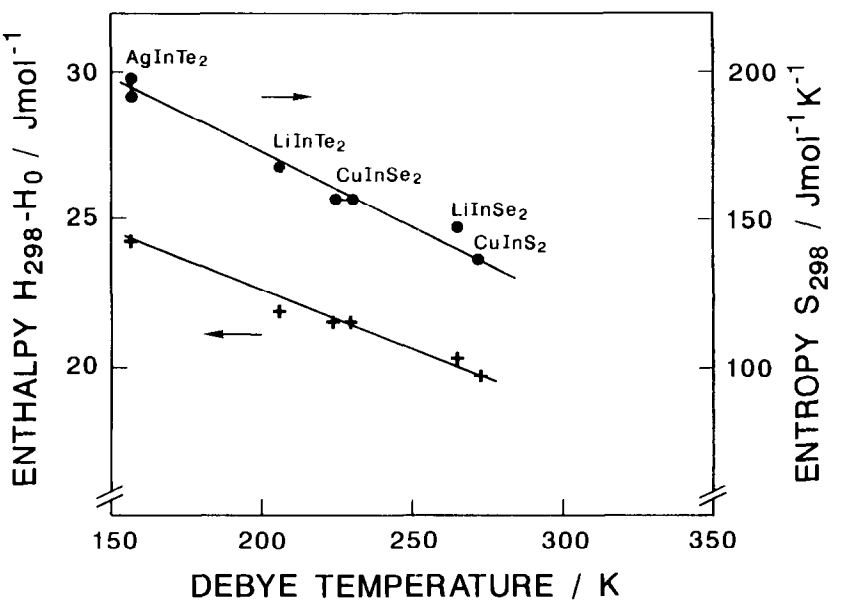

Fig. 8. Molar standard enthalpies and entropies of some chalcogenides as depending on the Debye temperature θ_D.

weight. Beside that exception the present data for $LiInSe_2$ and $CuInSe_2$ interpolate well with the other chalcogenides in that scheme. As considered above, we attribute this deviation basically to the low temperature Schottky-anomaly generated by the split position of the Li atom. The entropies of the Li compounds reconcile with the other chalcogenides within a few percent when we assume averaged entropy data as derived from the straight-line data in Fig. 8 and then add the entropy of a two-level Schottky-term with $\Delta S = 5.76\,J\,(mol\,K)^{-1}$. The outlined scheme together with the data collected in Table 2 and Fig. 6 enable calculation of reliable thermodynamic values for the not yet calorimetrically investigated chalcogenides with inaccuracies of less than 3%.

5. Conclusion

Calorimetric studies of $LiInSe_2$ and $CuInSe_2$ and accompanying studies on literature specific heat (C_p) data of other chalcogenides reveal anomalous low temperature heat contributions in Li chalcogenides. We demonstrate that the specific heats, and therefore the thermodynamic functions of chalcogenides, are describable by a generalized formula for $C_p(T)$ that is normalized to the 0 K Debye temperature θ_0. The specific heat of $LiInSe_2$ displays an additional contribution at low temperatures that is suggested to originate from a two-level Schottky system due to the split position of the Li atom.

Acknowledgements

The authors thank Dr. Dieter Oppermann, Leipzig, for providing the samples of $LiInSe_2$ and $CuInSe_2$.

References

[1] A.F. Wells, Structural Inorganic Chemistry, Clarendon Press, Oxford 1984.
[2] W. Hönle, G. Kühn and H. Neumann, Z. anorg. allg. Chem., 543 (1986) 161.
[3] W. Hönle, G. Kühn and H. Neumann, Z. anorg. allg. Chem., 532 (1986) 150.
[4] K.S. Knight, Mater. Res. Bull., 27 (1992) 161.
[5] S.C. Abrahams and F.S.L. Hsu, J. Chem. Phys., 63 (1975) 1162.
[6] K.J. Bachmann, F.S.L. Hsu, F.A. Thiel and H.M. Kasper, J. Electron. Mater., 6 (1977) 431.
[7] K. Bohmhammel, P. Deau, G. Kühn and W. Möller, Phys. Stat. Sol. (a), 71 (1982) 505.
[8] G. Kühn, E. Pirl, H. Neumann and E. Nowack, Cryst. Res. Technol., 22 (1987) 265.
[9] H. Neumann, G. Kühn and W. Möller, Phys. Stat. Sol. (b), 144 (1987) 565.
[10] U.-C. Boehnke, G. Kühn, F.I. Frolova, I.E. Paukov and H. Neumann, J. Therm. Anal., 33 (1988) 205.
[11] U.-C. Boehnke and G. Kühn, J. Mater. Sci., 22 (1987) 1635.
[12] T. Kamijoh and K. Kuriyama, J. Cryst. Growth, 51 (!981) 6.
[13] E. Gmelin and P. Rödhammer, Rev. Sci. Instrum., 14 (1981) 223.
[14] E. Gmelin, Thermochim. Acta, 110 (1986) 183.
[15] E. Gmelin and K. Ripka, Cryogenics, 21 (1981) 117.
[16] Lake-Shore Cryotronics, Westerville, Ohio 43081, U.S.A., Germanium resistor, type CR1000, No. 6565, calibrated according to IPTS-68.

[17] Rosemount Inc., Minneapolis, Minnesota 55435, U.S.A., Platinum resistor, type 118MF, calibrated according to IPTS-68.
[18] R.N. Goldberg and R. Weir, Pure Appl. Chem., 64 (1992) 1545.
[19] E. Gmelin, A. Simon, E. Brämer and R. Villar, J. Chem. Phys., 76 (1982) 6256.
R. Santandrea, E. Gmelin, C. Santandrea and H.G. von Schnering, Thermochim. Acta, 67 (1983) 263.
[20] G. Kühn, B. Schumann, D. Opfermann, H. Neumann, and H. Sobota, Z. anorg. allg. Chem., 531 (1985) 61.
[21] E. Gmelin, W. Hönle, Ch. Mensing and H.G. von Schnering, J. Therm. Anal., 35 (1989) 2509.
[22] V. Narayanamurthi and R.O. Pohl, Rev. Mod. Phys., 42 (1970) 201.
[23] S. Fiecher and E. Gmelin, Thermochim. Acta, 87 (1985) 319.
[24] E.S.R. GOPAL, Specific heats at low temperatures, Plenum Press, New York 1966.